

## Dynamic crack propagation in elastic-plastic solids under non-K-dominance conditions \*

X. DENG \*\*, A. J. ROSAKIS \*\*\* and S. KRISHNASWAMY \*\*\*\*

**ABSTRACT.** — This paper presents the results of a detailed study of dynamic crack propagation in elastic-plastic solids under non-K-dominance conditions, under which the singular elastic term, characterized by the dynamic stress intensity factor  $K$ , is not dominant around the crack-tip plastic zone. This study was carried out with the finite element method, using a multi-term boundary-layer formulation, under the restrictions of mode I, plane stress, and steady-state crack growth, and for both linear-hardening and elastic-perfectly plastic materials. The effects of the far-field, nonsingular elastic terms on the near-tip elastic-plastic field quantities are explored in terms of the variations of those quantities with respect to two parameters,  $\gamma_1$  and  $\gamma_2$ , which are, respectively, the ratios of the first and second nonsingular elastic terms to the singular term, of the stress component  $\sigma_{11}$ , at a certain distance ahead of the crack tip. Assuming a fracture criterion based on the attainment of a critical effective plastic strain value at a certain fixed distance ahead of the crack tip, the finite element results are used to derive critical values of  $K$  for various crack propagation speed  $v$ . It is found that the presence of a nonnegligible amount of nonsingular, higher-order terms in the elastic far fields, with  $\gamma_1$  and  $\gamma_2$  varying from  $-1.0$  to  $1.0$ , will cause a sensible amount of scattering in the theoretically predicted  $K-v$  values (with a maximum around 20% in comparison with that obtained under K-dominance conditions), which is, however, still well within that obtained from experimental measurements.

### 1. Introduction

The most popularly debated fracture criterion for dynamic crack propagation is stated as  $K(t) = K(v)$ , where  $t$  and  $v$  denote, respectively, the time and the speed of crack propagation, and  $K$  is a generic symbol for the dynamic stress intensity factor, which characterizes the singular elastic crack-tip fields. On the left-hand side of the criterion is the instantaneous value of  $K$  attained during an actual crack propagation event, and on the right-hand side is the critical value of  $K$ , or the dynamic fracture toughness, at a certain crack speed, which is regarded as a material property. Concerns about the appropriateness of this fracture criterion have been centered around the uniqueness of the dependence of  $K$  on  $v$ , and a substantial amount of research in dynamic fracture

\* Based on an original research report by the authors (GALCIT REPORT SM90-14, California Institute of Technology, Pasadena, California, U.S.A., 1990).

\*\* Department of Mechanical Engineering, University of South Carolina, Columbia, SC 29208, U.S.A.

\*\*\* Graduate Aeronautical Laboratories 105-50, California Institute of Technology, Pasadena, CA 91125, U.S.A.

\*\*\*\* Department of Mechanical Engineering, Northwestern University, Evanston, IL 60208, U.S.A.

has been directed towards the determination of the  $K$  vs.  $v$  relationship. For crack propagation in elastic-plastic materials that fail in a locally ductile manner, *i.e.*, by means of void nucleation, growth and coalescence,  $K-v$  curves derived from experimental measurements appear to show a one-to-one correspondence between  $K$  and  $v$  (*see* [Kobayashi & Dally, 1980]; [Rosakis *et al.*, 1984] and [Zehnder & Rosakis, 1990], among others), which are also confirmed by the results of theoretical, elastic-plastic studies ([Freund & Douglas, 1982]; [Lam & Freund, 1985]; [Deng & Rosakis, 1991]) under certain restrictions, such as the small-scale yielding conditions. Such a one-to-one correspondence, or the uniqueness of the relationship between  $K$  and  $v$ , is essential to the aforementioned fracture criterion, since only then the  $K-v$  curve can be regarded as a material property and used in structural designs.

From what we know today, however, it is still too early to claim the uniqueness of the  $K-v$  relationship. Firstly, experimental data obtained so far all involve large scattering, which makes it unclear as to the exact value of  $K$  given a certain crack speed  $v$ . In particular, it is noted that certain tendencies in the scatterings were observed in a study by Kalthoff [1983] and were attributed to the specimen dependence of the  $K-v$  relationship. In an independent experimental study by Dahlberg *et al.* [1980], deviations from the uniqueness were observed at high load levels and they were found to be influenced by the height of the specimens. Secondly, there are uncertainties about the accuracy and reliability of many of the experimental data, in that they were usually interpreted assuming that the elastic singular fields characterized by  $K$  dominated over the region where the measurements were made. The most often used technique is the method of caustics (*see*, for example, Kalthoff *et al.* [1980] and Rosakis [1980]), which in fact is based directly on the assumption of  $K$ -dominance near the crack tip. In this connection we call attention to the study of Nigam & Shukla [1988], who revealed that the  $K$ -values obtained, on identical specimens under identical loading, but from two different methods, namely the methods of caustics and photoelasticity, were off by as much as 50%. More recently, the issue of  $K$ -dominance during dynamic crack propagation was examined by Krishnaswamy & Rosakis [1991] and Krishnaswamy *et al.* [1991], with the conclusion that the elastic singular term alone cannot adequately describe the state of deformation in the region where the caustics data are usually collected. Then, it is readily seen that the presence of non- $K$ -dominance condition, when the higher-order, nonsingular elastic terms are not negligible, will cause scatters in  $K$  values if they are derived from experimental measurements made by, say, the method of caustics.

To examine the appropriateness of the stress intensity factor-based fracture criterion for dynamic crack growth, and to establish its range of applicability, we have to investigate, besides the usual errors associated with an experimental technique, the major factors that contribute to the scattering of  $K-v$  values in experimental measurements. There are basically two groups of major contributing factors: one arising from improper interpretations of experimental measurements and the other being associated with the assumptions of the fracture criterion itself. The first group includes factors such as the assumption of  $K$ -dominance, the use of steady-state field expansions, and the omission of three-dimensional and large-scale yielding effects. For example, the study by Brickstad [1983] has shown that when large scale yielding is present, an energy based fracture

criterion can be used in combination with an elasto-viscoplastic analysis to produce a fracture toughness versus crack speed curve that does not show the type of specimen-height induced scatter seen in [Dahlberg *et al.*, 1980]. A key example of the second group of factors is that the critical value of  $K$  may not be exactly a material property, that is, it may, for example, depend on the geometry of the specimen, which is related to the presence of nonsingular, higher-order terms in the elastic far fields. However, it can be argued that when such dependence is weak the fracture criterion based on  $K$  can be treated, for practical purposes, as being independent of the specimen geometry.

Considering the various possibilities raised in the above, it is only natural for us to single out the different major factors and to examine the role of each of the factors in order to arrive at a conclusive decision as to the usefulness of the  $K$ -based fracture criterion. As such, the purpose of the current study is to concentrate on the first two leading terms in the expansion of the crack-tip elastic far fields, to assess their influence on the state of deformation within the crack-tip elastic-plastic zone, and to predict theoretically the range of scatters in  $K-v$  values due to those two leading higher-order terms, with comparison to those obtained experimentally. This study is carried out with the finite element methods and under conditions of mode I plane stress and steady-state crack growth. (The steady-state assumption is necessary to facilitate a finite element study of this nature. However, since in this study we are concerned with the perturbations in the crack-tip elastic-plastic zone caused by disturbances in the surrounding elastic far fields, this assumption appears to be acceptable. The effects of any additional perturbations due to transient terms must be studied by modelling actual crack propagation events, which is computationally prohibitive, if not impossible, at the present time.) A brief formulation of the problem is given below.

## 2. Problem formulation

As shown in Figure 1, consider a crack propagating rapidly yet steadily along a straight path in a sheet made of an elastic-plastic material, where  $v$  is the crack speed which is a constant. The material obeys the  $J_2$  flow theory of plasticity and is either elastic-perfectly plastic or a linear hardening solid with a bilinear uniaxial stress-strain curve, where the slope of the elastic line is given by the Young's modulus  $E$  and that of the hardening line is given by  $E_r$ . (In this study, the elastic-perfectly plastic case is modelled by setting the ratio,  $E_r/E$ , denoted by  $\alpha$ , to zero.) An Eulerian-type finite element technique [Dean & Hutchinson, 1980] is adopted, such that a mesh of fixed size translates with the crack tip, and the boundary conditions are specified according to a multi-term boundary layer concept ([Larsson & Carlsson, 1973]; [Rice, 1974]).

Because of symmetry about the  $x$ -axis, only the upper half-plane is modelled here. A schematic of the finite element mesh is depicted in Figure 2, where the coordinates are normalized by  $(K/\sigma_0)^2$ ,  $\sigma_0$  being the material's initial yield stress in uniaxial tension. The domain under consideration has a non-dimensional size of  $9 \times 4.5$ , with the crack tip located at the mid-point of the bottom line. For comparison, the nondimensional size of the active plastic zone ahead of the crack tip will be on the order of 0.25. The

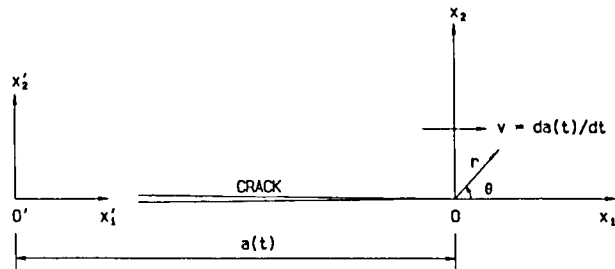


Fig. 1. — A diagram of crack growth, where  $(x'_1, x'_2)$  is a fixed reference system, and  $(x_1, x_2)$  is a moving system with origin at the crack tip,  $r$  and  $\theta$  being the associated polar coordinates.

whole mesh is composed of 1800 elements, and the ratio of the active plastic zone size to that of the smallest near-tip element is of the order of  $1.6 \times 10^4$ , which is designed to capture the correct asymptotic feature of the crack tip fields. To overcome numerical convergence difficulties associated with this extremely fine mesh focused around the crack tip, a solution procedure proposed in ([Deng, 1990]; [Deng & Rosakis, 1990]) is used to integrate the incremental elastic-plastic constitutive laws. For more details of the finite element formulation and mesh design the reader is referred to ([D, 1990]; [D & R, 1990, 1991]). A Poisson's ratio of  $\nu=0.3$  is used in all calculations.

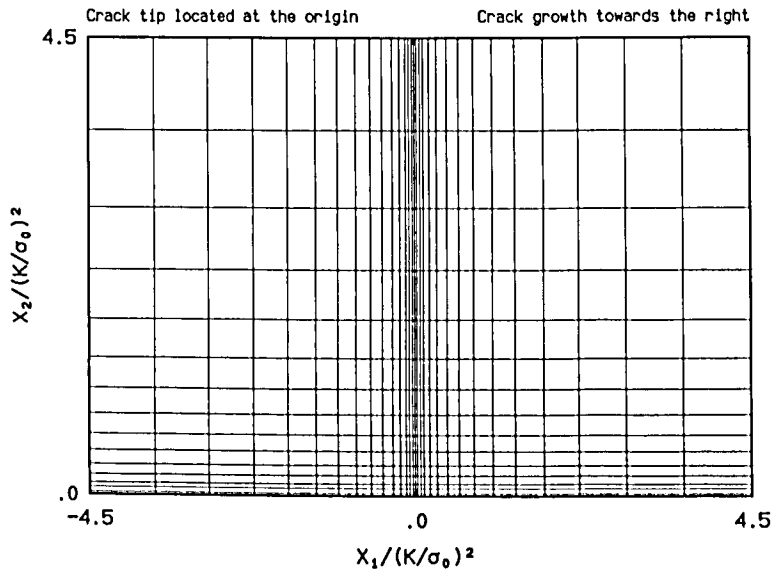


Fig. 2. — A coarse representation of the finite element mesh used in the present computation.

To analyze the effects of the higher-order elastic terms, the displacements or tractions corresponding to a truncated, Williams-type eigen-expansion of the steady-state, elastodynamic crack-tip fields [Nishioka & Atluri, 1983] are specified on the boundaries of the finite element mesh, which, for example, can be written in terms of the stress components  $\sigma_{ij}$  as:

$$\sigma_{ij}(r, \theta) = \frac{K}{\sqrt{2\pi r}} \hat{\sigma}(0)_{ij} + T \delta_{1i} \delta_{1j} + \dots$$

where the first term gives the singular elastic crack-tip field and is characterized by the stress intensity factor; the second term represents uniaxial tension or compression  $T$  along the  $x_1$ -axis, which is closely related to stress biaxiality ahead of the crack tip; and the rest of them includes the third and even higher-order terms in the expansion, which disappear as  $r$  approaches zero. In this study, attention is focused on the singular term and the next two nonsingular terms, which are parametrized in terms of parameters  $\gamma_1$  and  $\gamma_2$ , which are defined, respectively, as the ratios of the values of the second (first nonsingular) and third (second nonsingular) terms of the stress component  $\sigma_{11}$ , to that of the first (singular) term, at the point  $\theta=0^\circ$  and  $r=L(K/\sigma_0)^2$ , where  $L$  is a dimensionless constant and is chosen to equal 4.5, the normalized size of the finite element mesh used in this study (for comparison, the active plastic zone size is typically on the order of 0.25). A spectrum of  $\gamma_1$  and  $\gamma_2$  values are selected from the range of  $[-1, 1]$ , which covers the cases from those where the K-controlled singular term is dominant at the point  $\theta=0^\circ$ ,  $r=L(K/\sigma_0)^2$ , to those where all the three terms are equally significant at that point.

### 3. Results and discussions

Before the results of this study are presented and discussed with confidence, it must be pointed out that the reliability and accuracy of the finite element procedures used here have been tested carefully in several ways. In particular, the reliability of this study is tested by checking the convergence of the results near the crack tip from one mesh to another and along different angular contours around the crack tip, and the accuracy is tested by comparing the results of this study with others available from the literature. Both tests are done for small-scale yielding cases only, since they differ from the present case only in the prescribed boundary-layer conditions.

Shown in Figure 3 are comparisons published earlier by two of the authors [D & R, 1991] for the case of plane stress, quasi-static crack growth in elastic-perfectly plastic solids. Angular stress variations in Figure 3(a) are drawn from two different crack-tip circular contours of two different finite element meshes (one with 1 800 elements and the other with 4 050 elements). The contour represented by a constant radial distance to the crack tip,  $r/(K/\sigma_0)^2=0.6411 \times 10^{-3}$ , is from the coarser mesh which is also used in this study, and the contour with  $r/(K/\sigma_0)^2=0.2033 \times 10^{-3}$  is from the finer mesh, which is computationally much more expensive. Convergence of our finite element solution is obvious. Also shown in this figure is the result of a study by Narasimhan *et al.* [1987] using a totally different finite element formulation. The angular stress variations from these authors are drawn from a rectangular rather than circular contour around the crack tip, resulting in some deviation from our results. Nonetheless, the comparison is excellent, which can also be seen from the radial dependence of the stresses along the crack line, as shown in Figure 3(b), where  $\tau_0$  is the initial yield stress in pure shear.

Figures 4 and 5 demonstrate the remarkable accuracy of the finite element procedure used in this study by comparing the angular variations of the stress and velocity components at the crack tip with those obtained from asymptotic analyses. For the case

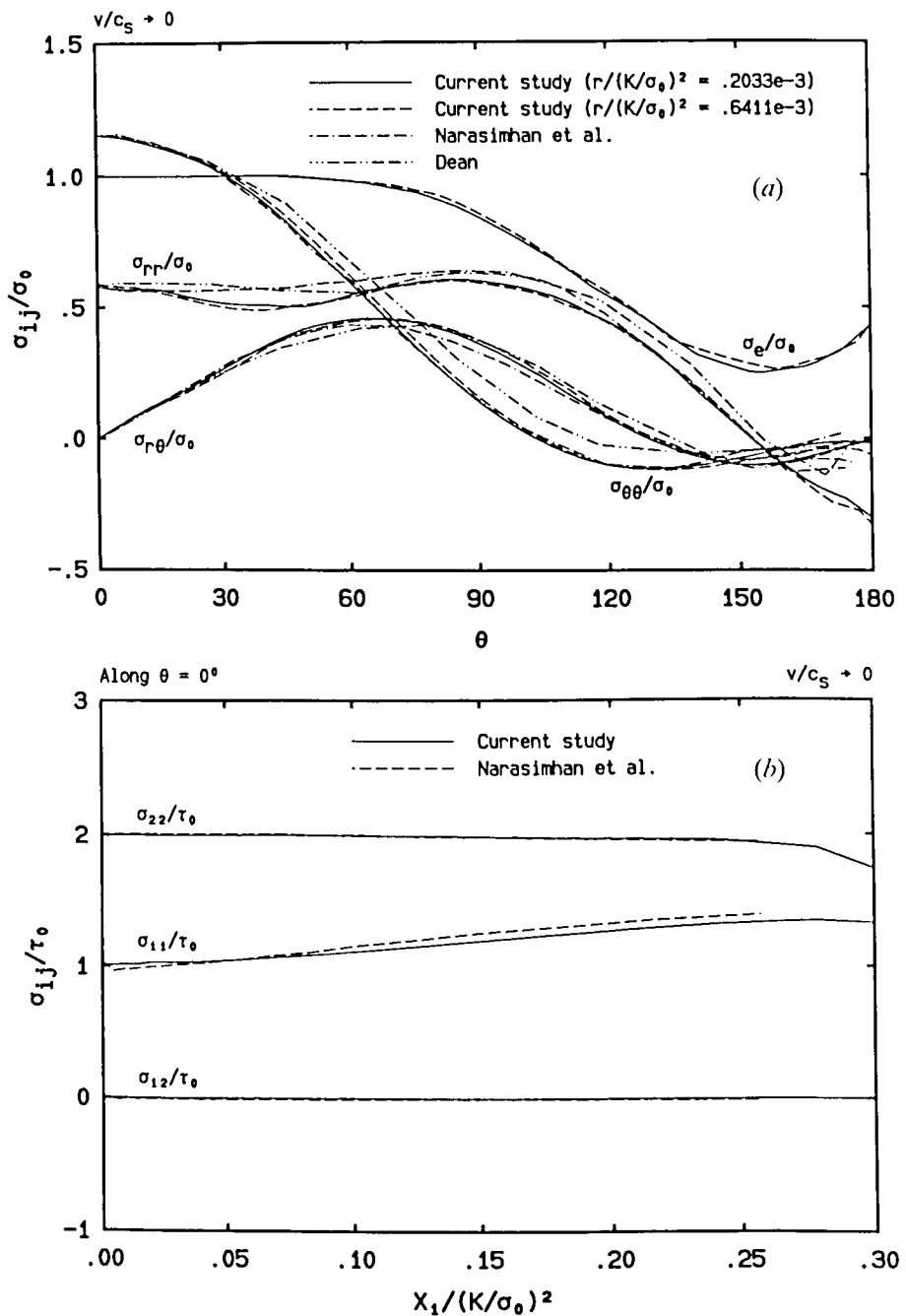


Fig. 3. - (a) Angular variations of the effective stress and the polar stress components along two different circular paths, compared with the results by Narasimhan *et al.* [1987]; (b) Detailed view of the radial dependence of the stress components at crack front, compared with the results by Narasimhan *et al.* [1987].

of mode I crack growth in linear hardening materials under plane stress conditions, asymptotic studies have been carried out by Amazigo & Hutchinson [1977] and Ponte

Castañeda [1987] for quasi-static crack growth, and by Achenbach *et al.* [1981] and Östlund [1991] for dynamic crack growth. The comparisons here were originally reported in [D & R, 1992*a*] and are made with the results of Ponte Castañeda [1987] for the quasi-static case, as shown in Figure 4(*a*) and 4(*b*), and with Achenbach *et al.* [1981] for the dynamic case, as shown in Figure 5. We point out that it does not matter that different Poisson's ratio values are used in our study and [P, 1987] because the crack tip deformation is dominated by incompressible plastic strains. We also note that the asymptotic solution in [A, 1981] stops at the elastic-plastic boundary, which is indicated by the start of deviation of the effective stress  $\sigma_e$  from the flow stress  $\sigma$ . In any case, the agreement between the finite element solutions and those of the asymptotic analyses is seen to be very good. The same conclusion can be reached if comparisons are made between the finite element solutions and those of the other two studies. More comparisons, for the case of plane stress crack growth in power-law hardening materials, can be found in [Deng & Rosakis, 1992*b*].

In what follows, discussions are given for the effects of the higher-order terms on the crack-tip active plastic zone and the angular and radial field variations, and on the  $K$  vs.  $v$  relationship, which is derived theoretically assuming a fracture criterion based on the attainment of a critical effective plastic strain at certain distance ahead of the crack tip. Finite element computations have been performed for various values of the crack speed  $v$  and hardening parameter  $\alpha$ , but for the sake of brevity, only those for  $v=0.3c_s$  ( $c_s$  being the material's shear wave speed) and  $\alpha=0.4$  and  $0.0$  will be presented here, which however are often typical of the other results. Also to save space, most results given here are for extreme values of  $\gamma_1$  and  $\gamma_2$  only, namely  $-1, 0, 1$ . All angular field variations are abstracted from the finite element data along a crack-tip circular path of radius  $r=0.6411 \times 10^{-3} (K/\sigma_0)^2$ .

### 3.1. THE ACTIVE PLASTIC ZONE AND ELASTIC-PLASTIC FIELD VARIATIONS

As shown in Figures 6(*a*) and 7 for  $\alpha=0$  and Figures 6(*b*) and 8 for  $\alpha=0.4$ , for various combinations of the extreme values of  $\gamma_1$  and  $\gamma_2$ , the higher-order nonsingular elastic terms have significant influence on the overall size and shape of the crack-tip active plastic zone. But, interestingly, their effect on the near-tip shape of the plastic zone is very limited; in fact, the angular extent of the active plastic zone at the crack tip appears to remain the same.

In clear contrast to the effect of  $\gamma_1$  and  $\gamma_2$  on the plastic zone, the angular variations of the asymptotic elastic-plastic crack-tip fields are only affected slightly by the higher-order elastic far-field terms. The angular dependence of the polar stress components are plotted in Figures 9 and 10 for  $\alpha=0.4$  and at a small distance of  $r=0.6411(10)^{-3} (K/\sigma_0)^2$  to the crack tip, from which we see hardly any sign of the presence of the higher-order terms. As to the plastic strain components, it is found that their actual angular variations remain the same when  $\gamma_1$  and  $\gamma_2$  are not zero, but their amplitudes do vary at different  $\gamma_1$  and  $\gamma_2$  values. For example, when  $\gamma_2$  is zero, the amplitude variations with  $\gamma_1$  are small (not shown here), but when both  $\gamma_1$  and  $\gamma_2$  take their positive or negative limiting values, the variations can go above 7% relative to the case of K-dominance, as shown in Figure 11 for  $\alpha=0$ , which is the worst case. In general,

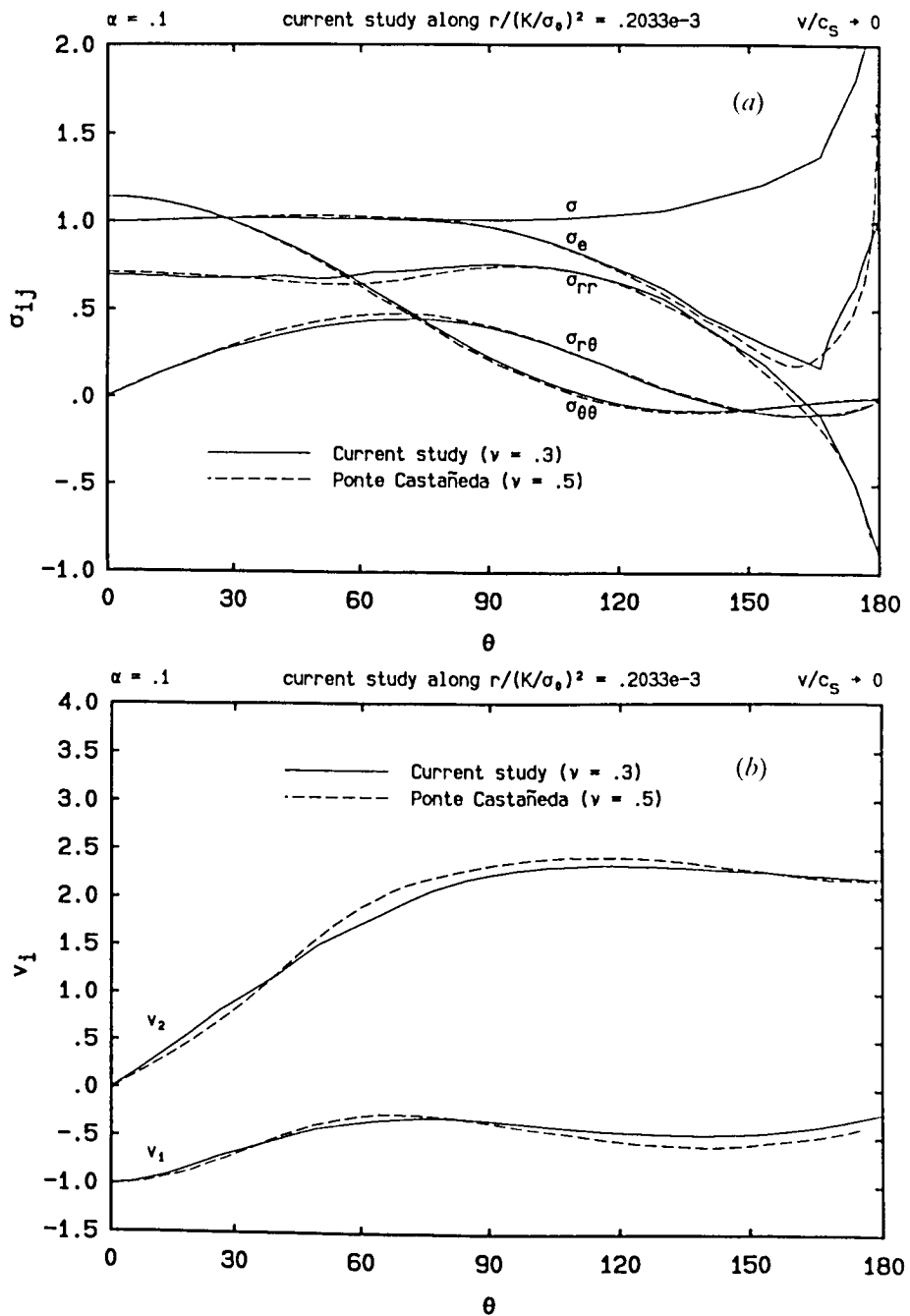


Fig. 4. — A comparison of angular stress and velocity fields for  $\alpha=0.1$  with the asymptotic solutions by Ponte Castañeda [1987]; (a) Polar stress components, the effective stress  $\sigma_e$ , and the flow stress  $\sigma$ , normalized such that  $\sigma_e = 1$  at  $\theta=0$ ; (b) Cartesian velocity components, normalized such that  $v_1 = -1$  at  $\theta=0$ .

the plastic strain curves associated with the same  $\gamma_1$  value are found to be very close to each other, suggesting that the effect of  $\gamma_1$  dominates that of  $\gamma_2$  in angular strain



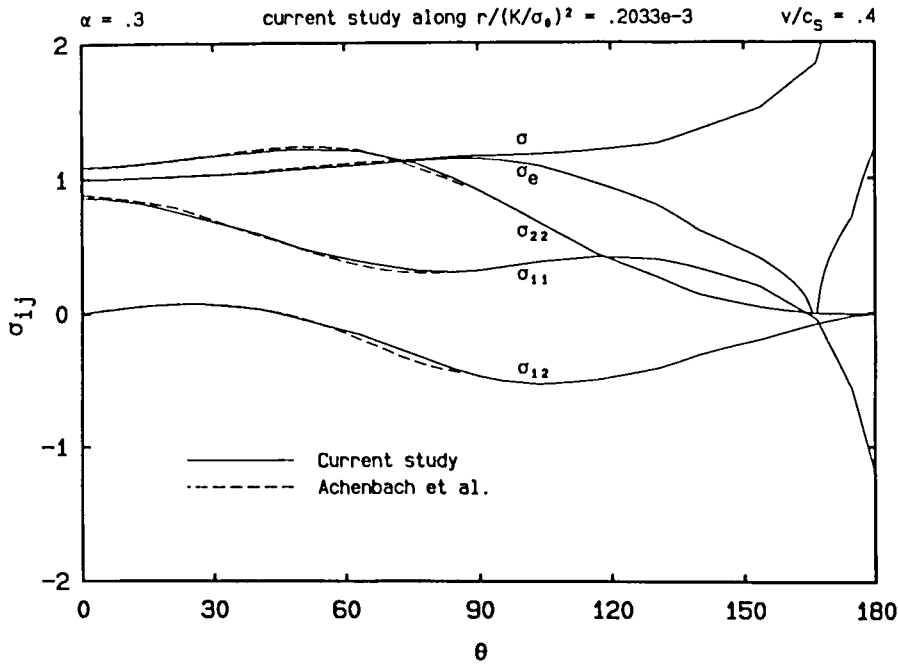


Fig. 5. - Angular variations of the polar stress components, the effective stress  $\sigma_e$ , and the flow stress  $\sigma$  for  $\alpha=0.3$  and  $v/c_s=0.4$ , normalized such that  $\sigma_e=1$  at  $\theta=0$ , with comparison to the asymptotic solution by Achenbach *et al.* [1981].

distributions. This tendency is even stronger in the angular variations of the rectangular velocity component  $v_1$  for different  $\gamma_1$  and  $\gamma_2$  values. To illustrate clearly the trend in the angular velocity variations, the effect of  $\gamma_1$  alone is shown in Figure 12, and the combined effect of  $\gamma_1$  and  $\gamma_2$  is shown in Figure 13, where the curves with  $\gamma_1=1$  overlap under the curve with  $\gamma_1=\gamma_2=0$ , and those with  $\gamma_1=-1$  overlap above the curve with  $\gamma_1=\gamma_2=0$ . It appears that this behavior has to do with the fact that during steady-state crack growth,  $v_1$  is related to the rectangular strain component  $\epsilon_{11}$  through  $v_1 = -v\epsilon_{11}$ , and that  $\gamma_1=1$  and  $-1$  correspond to, respectively, remote uniform tension and compression along the  $x_1$ -axis.

To get a sense of the degree of dependence of the stress and strain components on the nonsingular higher-order elastic terms at various distances from the crack tip, the radial variations of the crack-tip fields are examined in the following along the prospective crack line  $\theta=0^\circ$ . Shown in Figure 14 is the effect of  $\gamma_1$  alone on the rectangular stress components for the case of  $\alpha=0.4$ . The results demonstrate that when a tension ( $\gamma_1>0$ ) is added to the K-field on the far-field elastic boundary, the value of  $\sigma_{11}$  will be increased relative to that from a K-dominance solution, but when a compression ( $\gamma_1<0$ ) is applied,  $\sigma_{11}$  will be decreased, which is consistent with our intuition. Similar observations can be made for an elastic-perfectly plastic solid, whose initial yield stress in pure shear is denoted as  $\tau_0$ . As shown in Figure 15(a), the stress curves for  $\sigma_{11}$  are grouped above or below those for  $\gamma_1=\gamma_2=0$ , depending on whether  $\gamma_1$  is positive or negative. It is noted that the stress component  $\sigma_{22}$  has an opposite trend as  $\gamma_1$  varies from negative values to positive ones. This is because the yield surface for the case of  $\alpha=0$  is fixed and the

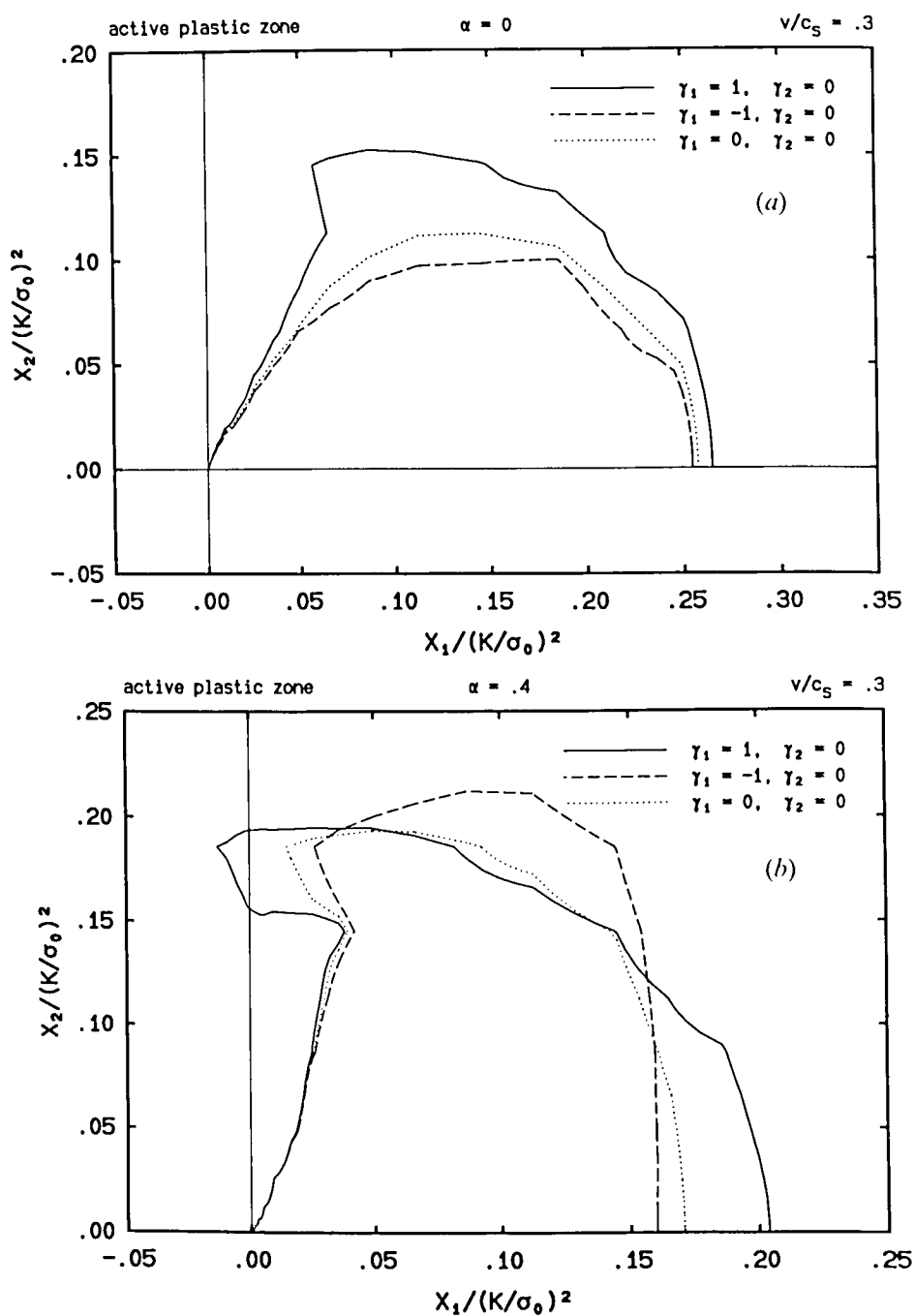


Fig. 6. — The effect of  $\gamma_1$  on the crack-tip active plastic zone for  $v/c_s = 0.3$ , plotted in normalized coordinates; (a)  $\alpha = 0$ , (b)  $\alpha = 0.4$ .

variation of  $\sigma_{22}$  must compensate that of  $\sigma_{11}$ . (However, when  $\alpha$  is not zero, for which the yield surface can expand, the tendencies of the two stress components are found to be the same, which can be seen, for example, from Fig. 14.) In all cases, at locations

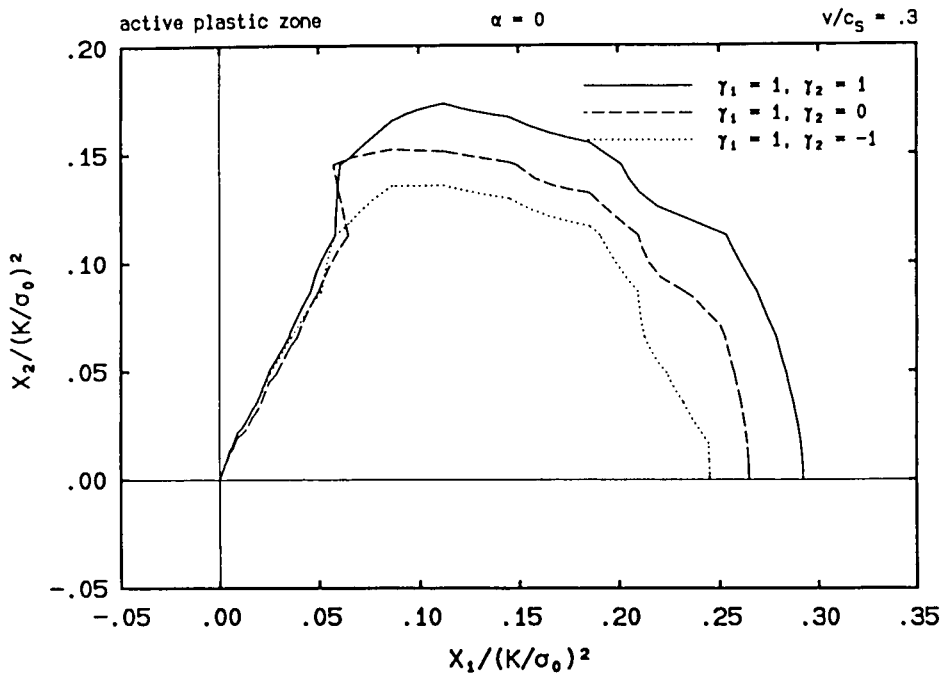


Fig. 7. - The effect of  $\gamma_2$ , with  $\gamma_1 = 1$ , on the crack-tip active plastic zone for  $\alpha = 0$  and  $v/c_s = 0.3$ , plotted in normalized coordinates.

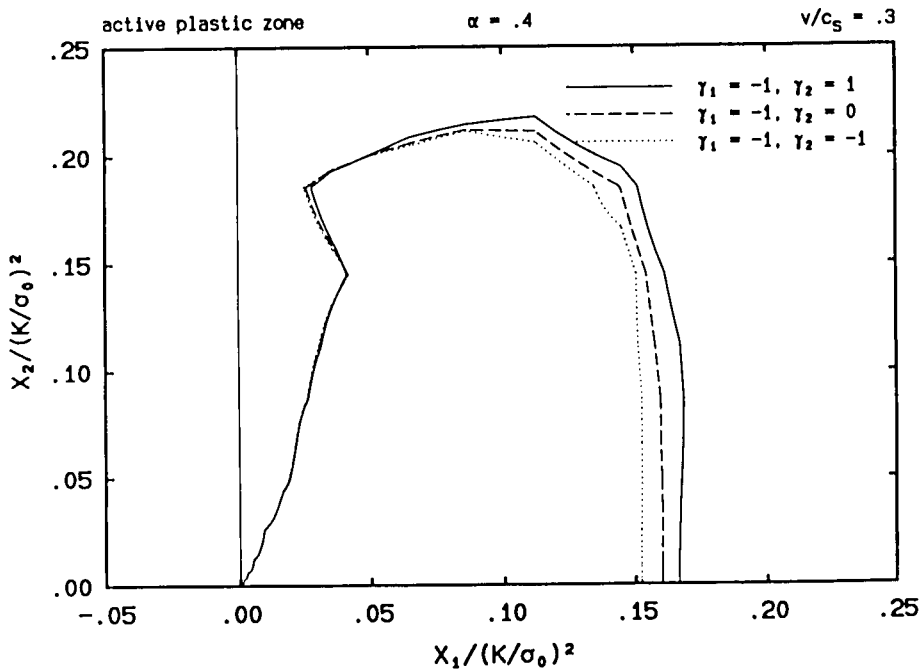


Fig. 8. - The effect of  $\gamma_2$ , with  $\gamma_1 = -1$ , on the crack-tip active plastic zone for  $\alpha = 0.4$  and  $v/c_s = 0.3$ , plotted in normalized coordinates.

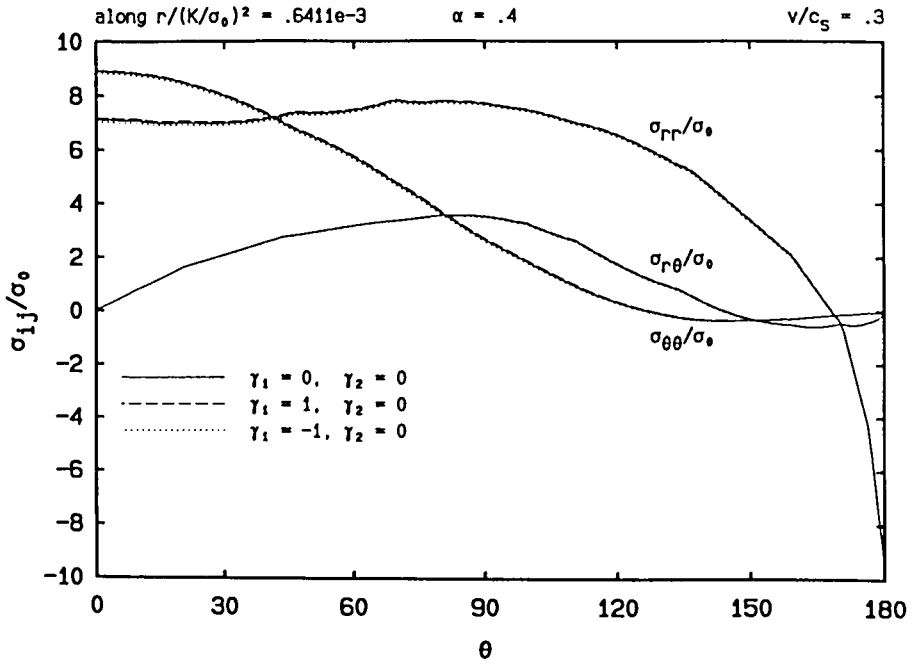


Fig. 9. — The effect of  $\gamma_1$  on the angular variations of the polar stress components for  $\alpha=0.4$  and  $\nu/c_s=0.3$ .

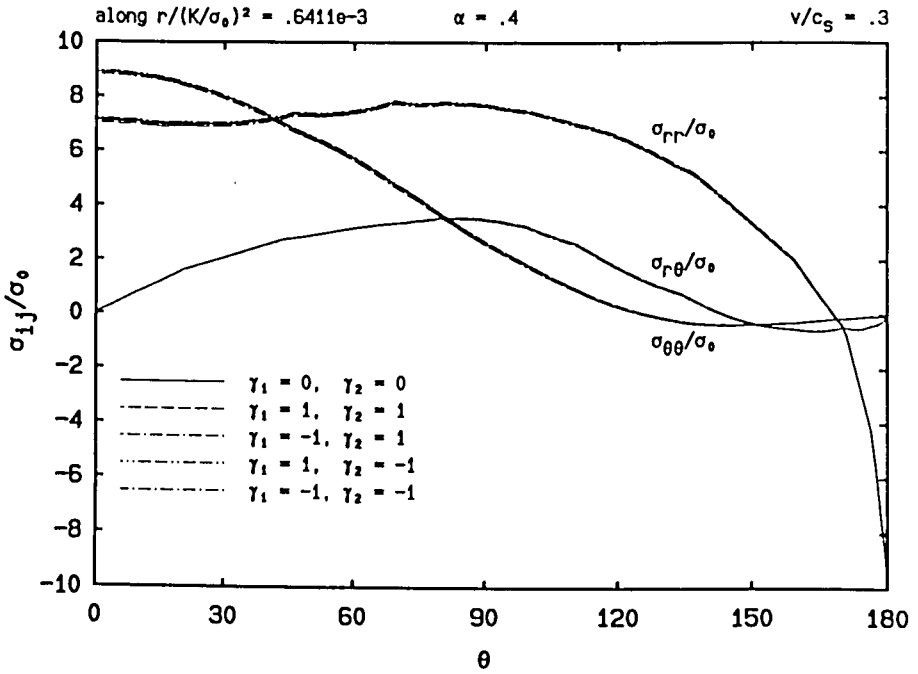


Fig. 10. — The combined effect of  $\gamma_1$  and  $\gamma_2$  on the angular variations of the polar stress components for  $\alpha=0.4$  and  $\nu/c_s=0.3$ .

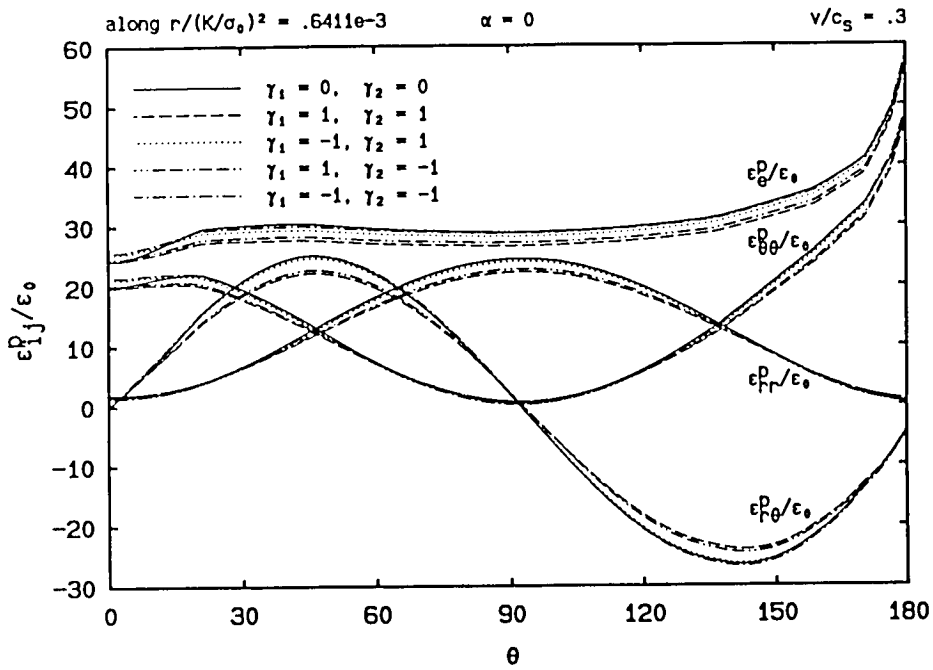


Fig. 11. — The combined effect of  $\gamma_1$  and  $\gamma_2$  on the angular variations of the effective plastic strain and the polar plastic strain components for  $\alpha=0$  and  $v/c_s=0.3$ .

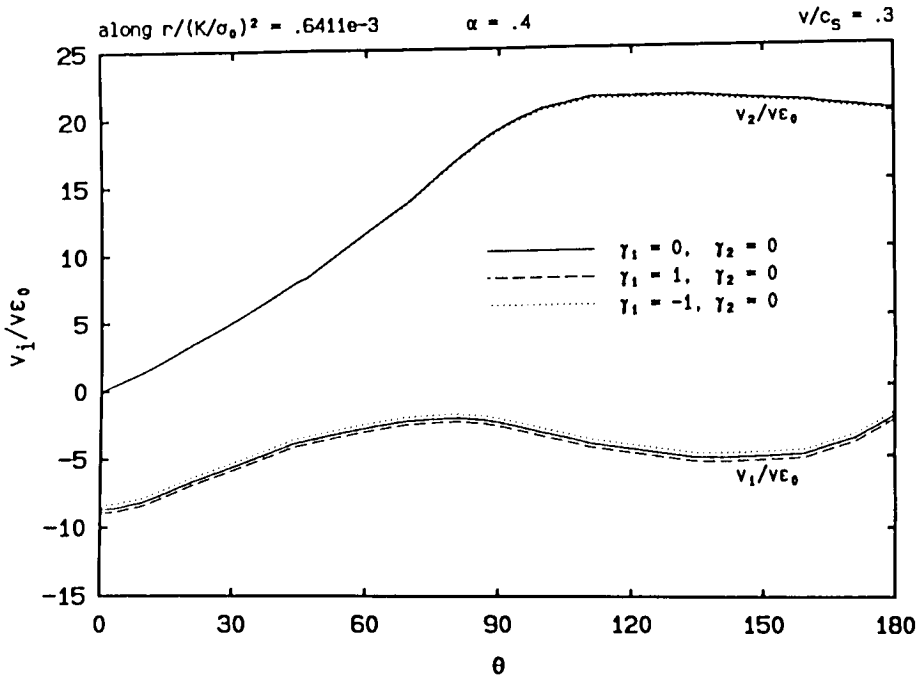


Fig. 12. — The effect of  $\gamma_1$  on the angular variations of the rectangular velocity components for  $\alpha=0.4$  and  $v/c_s=0.3$ ,  $\epsilon_0$  being the initial yield strain in uniaxial tension.

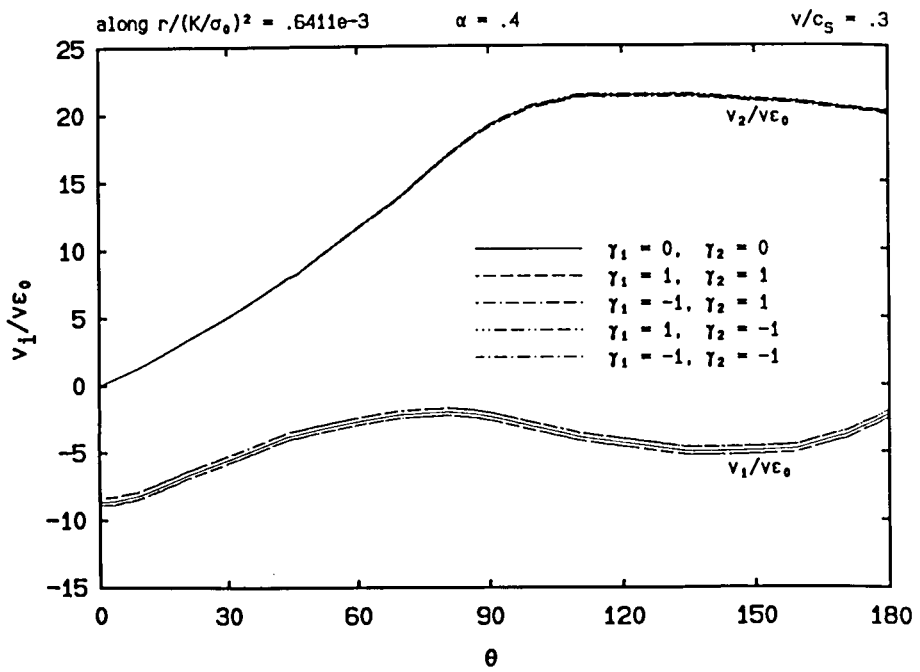


Fig. 13. — The combined effect of  $\gamma_1$  and  $\gamma_2$  on the angular variations of the rectangular velocity components for  $\alpha=0.4$  and  $v/c_s=0.3$ ,  $\epsilon_0$  being the initial yield strain in uniaxial tension.

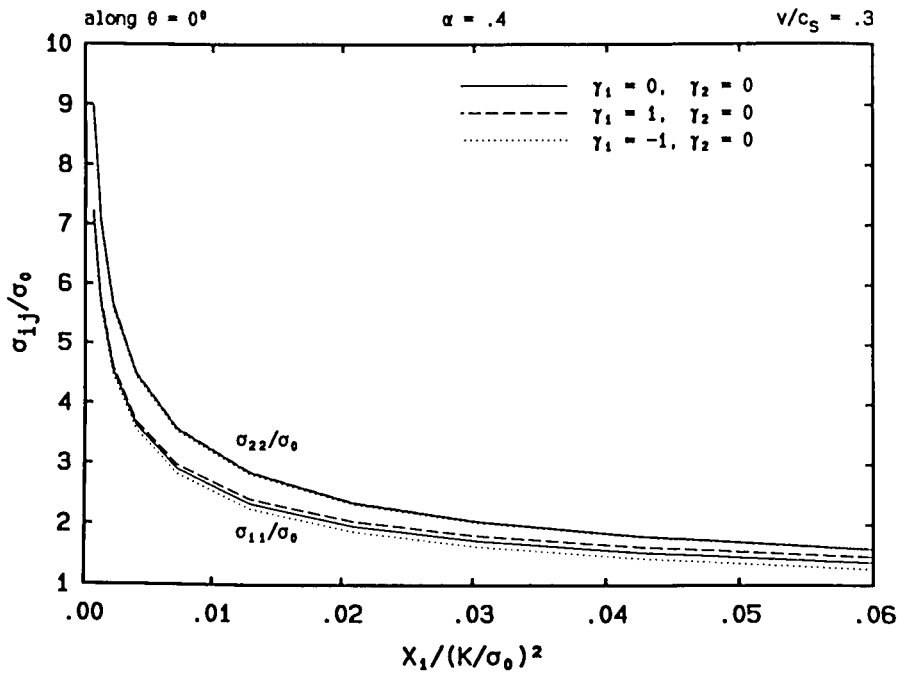


Fig. 14. — A detailed view of the effect of  $\gamma_1$  on the radial variations of the stress components for  $\alpha=0.4$  and  $v/c_s=0.3$ , plotted in the normalized coordinates.

sufficiently close to the crack tip, for example, when  $r < 0.6 (K/\sigma_0)^2$  [see Figs. 14 and 15(b)], the stress components are not much affected by the higher-order elastic terms.

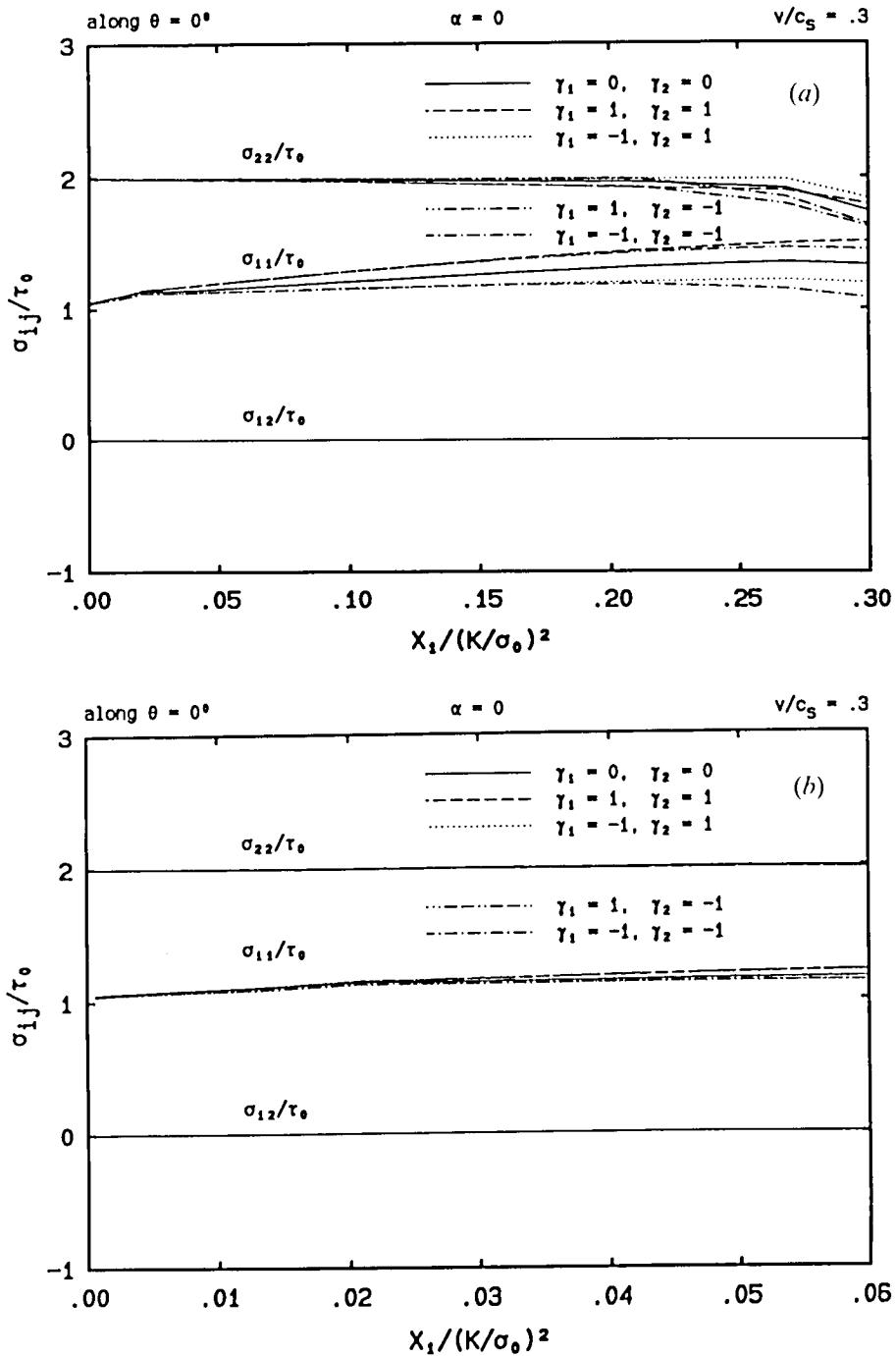


Fig. 15. - The combined effect of  $\gamma_1$  and  $\gamma_2$  on the radial variations of the stress components for  $\alpha=0$  and  $v/c_s=0.3$ , plotted in the normalized coordinates: (a) a global view; (b) a near-tip view.

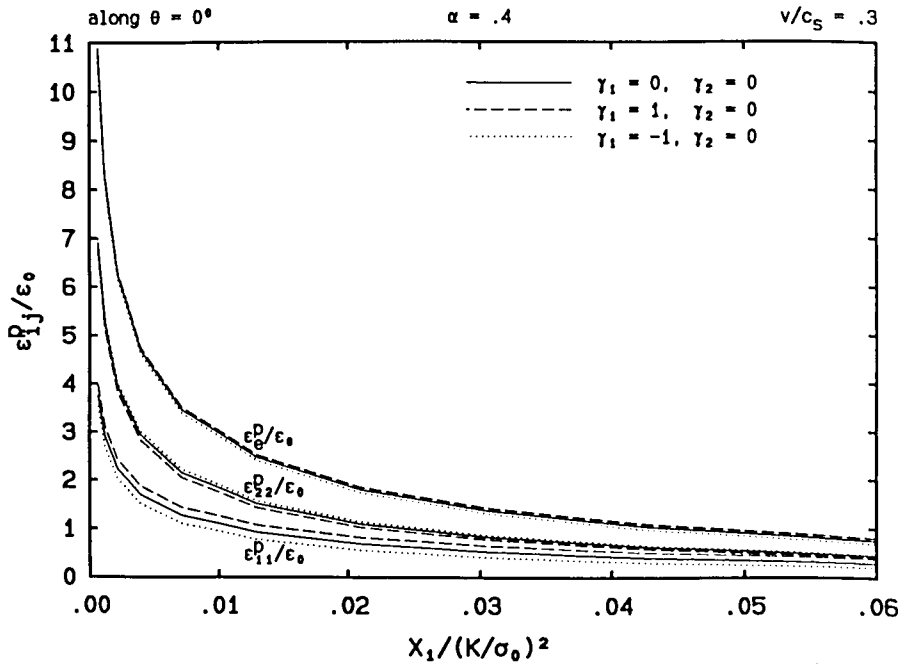


Fig. 16. — The effect of  $\gamma_1$  on the radial variations of the effective plastic strain and the plastic strain components for  $\alpha=0.4$  and  $\nu/c_s=0.3$ , plotted in the normalized coordinates.

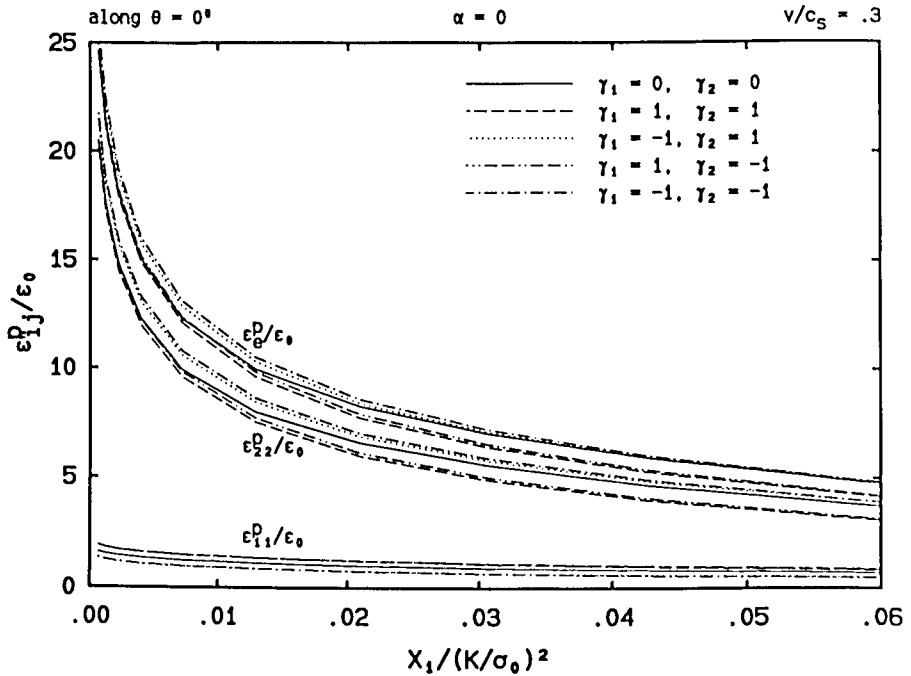


Fig. 17. — The combined effect of  $\gamma_1$  and  $\gamma_2$  on the radial variations of the effective plastic strain and the plastic strain components for  $\alpha=0$  and  $\nu/c_s=0.3$ , plotted in the normalized coordinates.



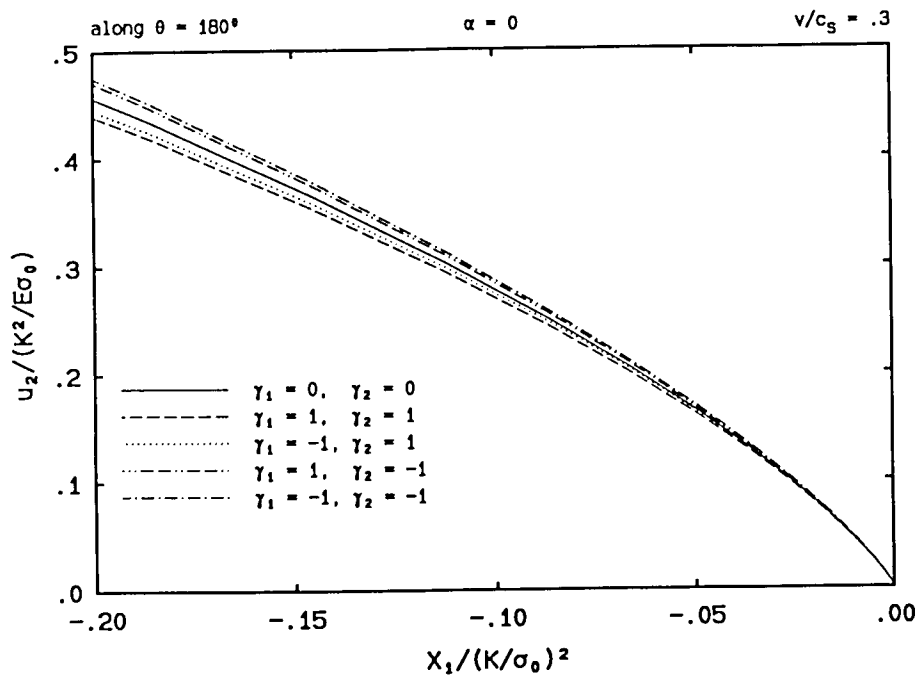


Fig. 18. - The combined effect of  $\gamma_1$  and  $\gamma_2$  on the radial variations of the vertical displacement component for  $\alpha=0$  and  $v/c_s=0.3$ , plotted in the normalized coordinates.

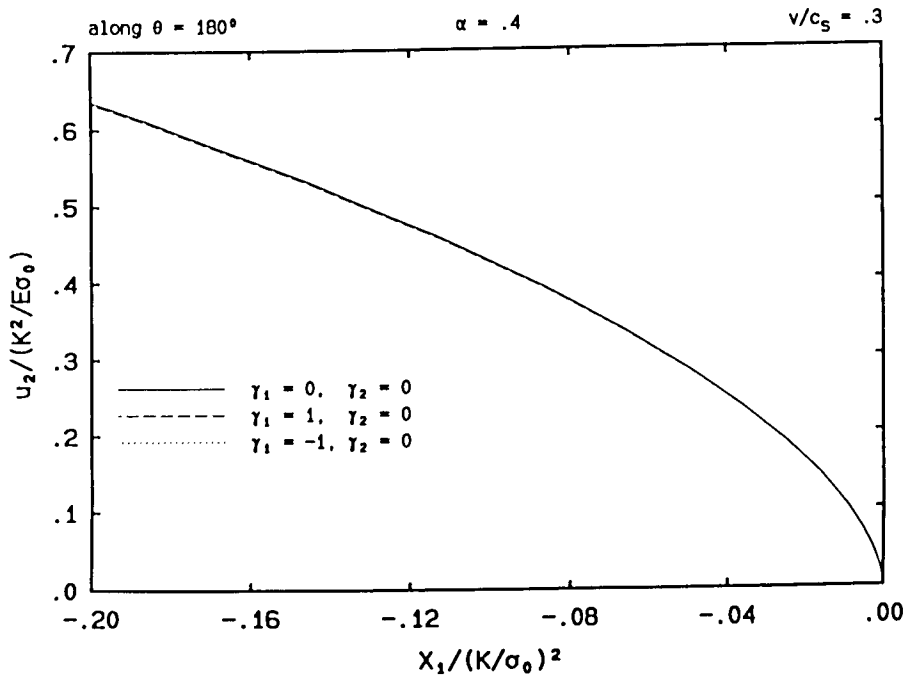


Fig. 19. - The effect of  $\gamma_1$  on the radial variations of the vertical displacement component for  $\alpha=0.4$  and  $v/c_s=0.3$ , plotted in the normalized coordinates.

The effects of the higher-order terms on the crack-tip plastic strains distributions are still small (*see Fig. 16*), although they appear to be more noticeable than those for the stresses. Again, as in stress variations, these plastic strain curves are grouped according to the value of  $\gamma_1$  (*see Fig. 17*), which is also consistent with earlier observations on the angular variations of strains and velocities. However, contrary to the above tendencies exhibited by the stress and strain variations, the crack-tip opening displacement (twice of the vertical displacement component) is seen to follow a trend dictated by  $\gamma_2$ , as illustrated in Figure 18, and the influence exerted by  $\gamma_1$  alone is negligible (*see Fig. 19*), which is expected since the direction of the displacement component in question is perpendicular to that of the tension or compression due to  $\gamma_1$  in the elastic far-field.

### 3.2. THE K vs. v RELATIONSHIP

In an earlier study [D & R, 1991] a procedure was devised, after that of [F & D, 1982], to generate from the finite element data theoretical K vs. v curves by assuming a critical effective plastic strain fracture criterion ([McClintock, 1956; 1958]; [McClintock & Irwin, 1964]). By setting the critical value of the effective plastic strain  $\epsilon_c^p$  to fifteen times that of the initial yield strain  $\epsilon_0$ , it was demonstrated that the one-parameter, theoretical K vs. v relationship was able to characterize the main features of the experimental measurements documented in ([R *et al.*, 1984]; [Z & R, 1990]) on their 4 340 steel plate specimens. To assess the influence of the nonsingular elastic terms on the theoretically generated K-v values, the procedure of [D & R, 1991] is repeated here for all cases studied, with  $\gamma_1$  and  $\gamma_2$  ranging from  $-1$  to  $1$ , and  $v/c_s$  from  $0.1$  to  $0.35$ . The critical effective plastic strain is set to  $\epsilon_c^p = 15\epsilon_0$ .

Shown in Figures 20 and 21 for an elastic-perfectly plastic solid are variations of K with respect to  $\gamma_1$ , while  $\gamma_2 = 0$ , at different normalized crack speed  $m = v/c_s$ , where  $K_{Ic}^d$ , the toughness, is the critical dynamic stress intensity factor in mode I, and  $K_{ss}$  is the steady-state fracture toughness for quasi-static crack growth under K-dominance conditions. It is found that the relative deviation of the dynamic fracture toughness from the case of K-dominance is around 4%, and it reaches the maximum of 14% when  $m = 0.1$  and  $\gamma_1 = 1$ , which can be attributed to the fact that the toughness is smallest there. When the second leading nonsingular elastic term is added to the far-field elastic boundary, the finite element calculation shows a further deviation of the toughness values from those obtained under K dominance conditions. Again, the maximum relative difference, about 22%, occurs when  $m = 0.1$  with  $\gamma_1 = \gamma_2 = 1$ .

To see the extent of the theoretically predicted scattering in the K-v values for  $\gamma_1$  and  $\gamma_2$  in the range of  $[-1, 1]$ , we have compiled in Figure 22 relevant data from references ([R *et al.*, 1984]; [Z & R, 1990]; [D & R, 1991]) and data from this investigation for all combinations of  $\gamma_1$  and  $\gamma_2$  values considered. It is observed that, even with the large scatters present, the K-v values do show a one-to-one, monotonically increasing tendency as v increases. Furthermore, it can be seen that although the scatter due to the nonsingular high-order elastic terms can be substantial, it is in general small compared with that of the experiments, implying that the higher-order terms alone may not account for all the scatters observed. It is necessary to point out that while it appears that the range of values for  $\gamma_1$  and  $\gamma_2$  covered in this study is quite large, the actual values

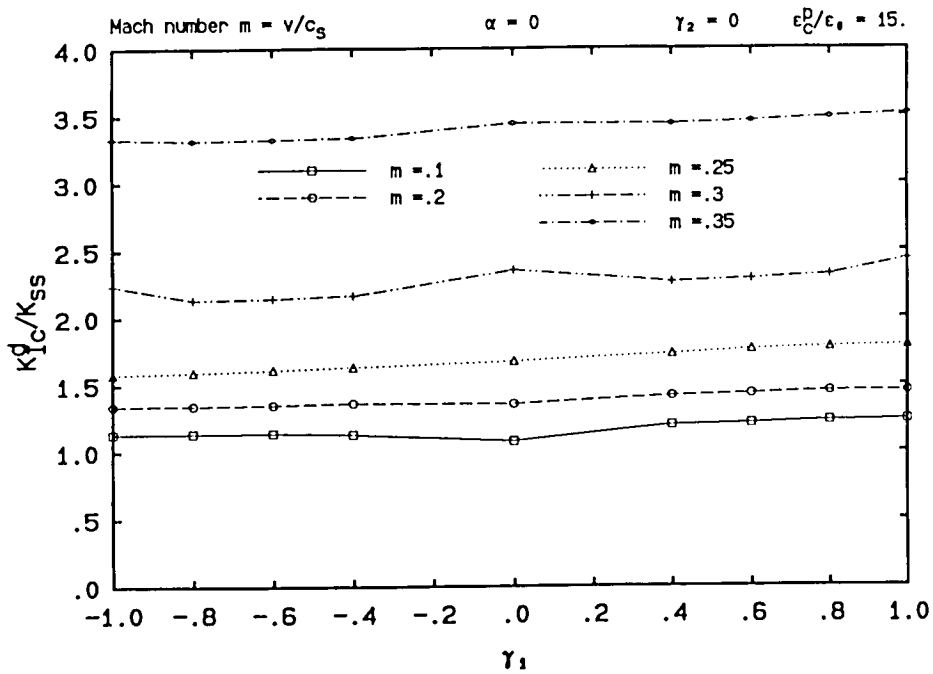


Fig. 20. - The variations of the normalized dynamic fracture toughness with respect to  $\gamma_1$  at various normalized crack propagation speed  $m = v/c_s$ .

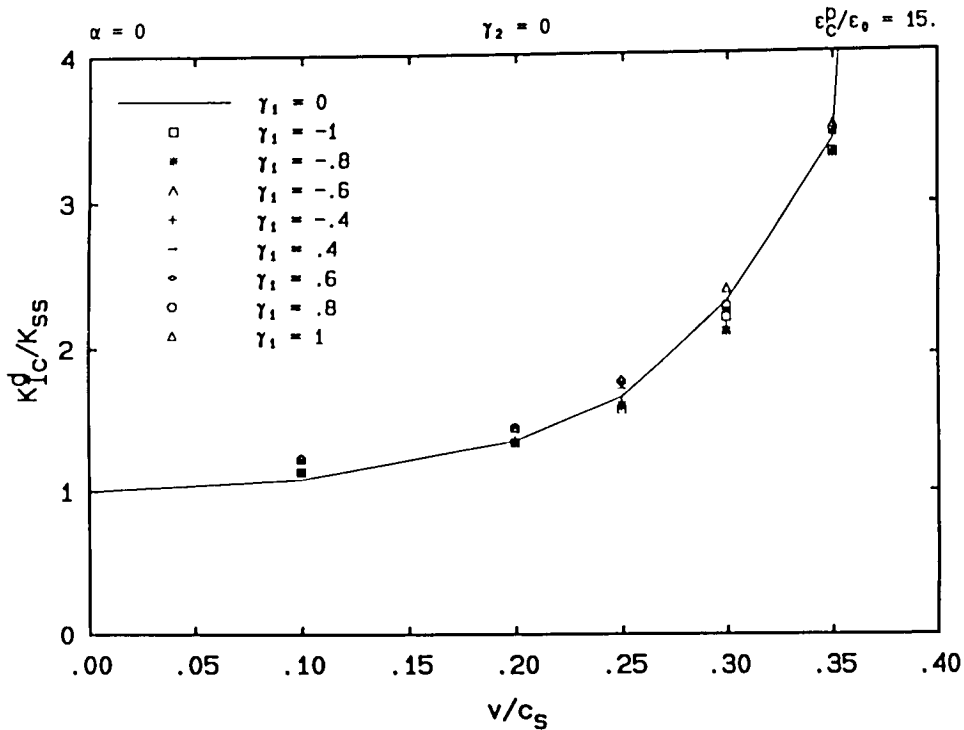


Fig. 21. - The effect of  $\gamma_1$  on the K vs. v relationship, plotted in normalized coordinates.

experienced by the two parameters during dynamic fracture tests are not clear, which introduces some uncertainties in interpreting the present results. To this end, we cite the findings of [L & C, 1973] for stationary cracks, from which  $\gamma_1$  and  $\gamma_2$  can be estimated to be within  $[-0.5, 0.3]$  for various common fracture specimens. Further, the value of  $\gamma_2$  is found to be around 0.1 from the results of a recent experimental study [Tippur *et al.*, 1991] on dynamic crack propagation. To obtain a realistic estimate for the higher-order terms for a particular dynamic crack propagation event, a detailed, reliable numerical simulation of the dynamic event must be conducted, with input of initial and boundary conditions from simultaneous measurements of the test. Nonetheless, it can be concluded from the results of the present multi-term boundary-layer study, that the higher-order elastic far-field terms do contribute to the scatters in the  $K-v$  values, but the extent of the scattering is still small compared to that observed in experimental measurements.

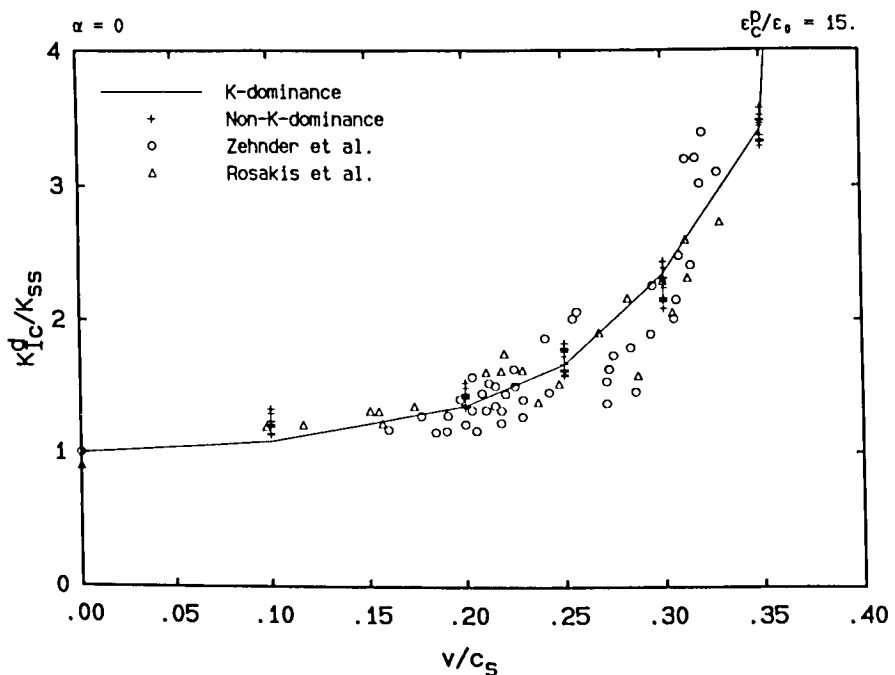


Fig. 22. — A comparison of scattering in theoretically generated and experimentally measured  $K$  values at different normalized crack speeds.

#### 4. Closing remarks

In the above, we presented the results of a detailed finite element study of steady dynamic crack growth in elastic-plastic solids under mode I plane stress and non-K-dominance conditions. The effects of the nonsingular, higher-order terms of the elastic far field on the deformation state within the crack-tip active plastic zone, and on the extent of scattering in dynamic fracture toughness values are investigated with respect to

parameters  $\gamma_1$  and  $\gamma_2$ . To summarize the major findings of this study, we observe the following key points:

(a) The size and shape of the crack-tip active plastic zone are strongly affected by the amount of the higher-order, nonsingular elastic far-field terms. This phenomenon is similar to those observed for plane strain problems, such as the case of dynamic crack growth in an infinite strip under large-scale yielding conditions studied by Östlund [1991].

(b) The elastic-plastic crack-tip fields are affected to different extent by the higher-order elastic terms, depending on the distance to the crack tip, but the extent is in general small compared with that for the plastic zone. Asymptotically, the effects of the nonsingular elastic terms on the elastic-plastic stress and strain fields are negligible at the crack tip.

(c) The scatter in  $K-v$  values caused by the first two leading nonsingular terms of the elastic far-field, for parameters  $\gamma_1$  and  $\gamma_2$  in the range of  $[-1, 1]$ , can be as high as 20% relative to the value for the K-dominance case for which  $\gamma_1 = \gamma_2 = 0$ . However, the amount of the theoretically predicted scattering, although appreciable, is still a fraction of that obtained from experimental measurements. Hence, when considered within the accuracy of today's experimental measurements, the dependence of the  $K-v$  relationship on higher-order elastic far-fields terms (which are related to factors such as the specimen geometry), as predicted by assuming a critical plastic strain-based fracture criterion, appears to be negligible.

At first sight, observations (b) and (c) appear to be somewhat inconsistent with each other, in that slight disturbances in the crack-tip elastic-plastic fields from the far-field higher-order elastic terms have led to quite sensible amount of scattering in the theoretically predicted  $K-v$  values. This inconsistency can be resolved if we note that the toughness values are derived from an effective plastic strain-based fracture criterion (*see* [D & R, 1991] for details of derivation) which tends to magnify differences present in the radial distributions of the plastic strains ahead of the crack tip. In this connection, we recall that the higher-order elastic terms indeed change the level of plastic straining along the prospective crack line (*see* Fig. 17).

In interpreting the above findings, we wish to call attention to the following facts. Firstly, the range of  $\gamma_1$  and  $\gamma_2$  values during dynamic fracture testings may exceed the one used in this study, and it is suggested that careful studies must be conducted for various types of specimens under actual test conditions in order to determine a realistic range for such parameters. Secondly, when K-dominance does not exist, the experimentally measured  $K$  values in Figure 22 are inaccurate, in that the method of caustics used in such experiments assumed the condition of K-dominance. However, the theoretically predicted  $K$  values are not affected. Finally, the parameters  $\gamma_1$  and  $\gamma_2$  in the finite element computation are defined at a fixed, *normalized* distance from the crack tip, which in fact corresponds to different physical distances for different  $K$  values. In this sense, an exact non-K-dominance condition is actually characterized by one more parameter, namely the physical location where the relative significance of the nonsingular elastic terms are defined. To this end, the present investigation only explored the effect of non-K-dominance for a set of sample points in the parametric space composed of  $\gamma_1$  and  $\gamma_2$  as well as  $L$ , the physical distance from the crack tip.

Further, it must be noted here that the situation cited in (b) and (c), especially regarding the effect of the T-stress and other higher-order terms on fracture toughness, is quite different from that experienced for plane strain problems. For example, for the case of dynamic crack growth in an infinite strip in plane strain, the study by Östlund [1991] clearly shows that geometric effects (equivalently, higher order terms) present under large-scale yielding conditions have a very strong influence on the crack-tip energy release rate, which will definitely affect the corresponding fracture toughness. To explain this difference from plane strain to plane stress, we have to note that both plane strain and plane stress conditions are idealized, two-dimensional approximations to the actual three-dimensional problem at the crack tip. From mathematical modelling point of view, it can be argued that the different effects of the higher-order elastic field terms on the near-tip inelastic fields and fracture parameters are caused by differences in constraint conditions placed on the two lateral surfaces of a plate, hence the differences in the governing equations, and by the material nonlinearity which prevents simple superposition of the crack-tip field quantities. To judge which approximation is more realistic near the crack tip, three-dimensional studies and physical arguments based on a thorough understanding of dynamic crack growth mechanisms will be needed.

In closing, we comment that further study is needed to establish firmly the dynamic stress intensity factor-based fracture criterion for dynamic crack growth under small-scale yielding conditions. Particularly, when conditions of K-dominance is not known to exist in advance, the interpretation of experimental measurements must be based on multi-term expansions of the elastic crack-tip fields that take care of the transient effects, such as those in ([Freund & Rosakis, 1992]; [Rosakis *et al.*, 1991]; [Deng, 1993; 1992c]; [Yang *et al.*, 1993]). What is more, the level of the higher-order terms relative to that of the singular term must be determined for various types of test specimens, so that factors essential to the practical application of the K-criterion, such as the dependence of  $K - v$  values on the specimen geometry, can be investigated and proper limitations can be placed on the application of the criterion. In cases where the specimen dependence is strong, a two-parameter fracture criterion based on K and, say T, must be pursued, as is done for the onset of crack growth in plane strain.

### Acknowledgements

This study was made possible by an ONR grant through contracts N00014-85-K-0596 and N00014-90-J-1340. The finite element computation was carried out on the supercomputers of the San Diego Supercomputer Center, which was made possible through the Presidential Young Investigator Award (NSF Grant MSM-84-51204) to AJR. Discussions with Dr. H. Tippur have been helpful.

### REFERENCES

- ACHENBACH J. D., KANNINEN M. F., POPELAR C. H., 1981, Crack-tip fields for fast fracture of an elastic-plastic material, *J. Mech. Phys. Solids*, **29**, 211-225.

- AMAZIGO J. C., HUTCHINSON J. W., 1977, Crack-tip fields in steady crack-growth with linear strain-hardening, *J. Mech. Phys. Solids*, **25**, 81-97.
- BRICKSTAD B., 1983, A viscoplastic analysis of rapid crack propagation experiments in steel, *J. Mech. Phys. Solids*, **31**, 307-327.
- DAHLBERG L., NILSSON F., BRICKSTAD B., 1980, Influence of specimen geometry on crack propagation and arrest toughness, *Crack arrest methodology and applications*, ASTM STP 711, American Society for Testing and Materials, 89-108.
- DEAN R. H., HUTCHINSON J. W., 1980, Quasi-static steady crack growth in small-scale yielding, Fracture mechanics, *Twelfth conference*, ASTM STP 700, American Society for Testing and Materials, I 39-I 51.
- DENG X., 1990, Dynamic crack propagation in elastic-plastic solids, *Ph. D. Thesis*, California Institute of Technology, Pasadena, California, USA.
- DENG X., ROSAKIS A. J., 1990, Negative plastic flow and its prevention in elasto-plastic finite element computation, *Finite Elements Anal. Design*, **7**, 181-191.
- DENG X., ROSAKIS A. J., 1991, Dynamic crack propagation in elastic-perfectly plastic solids under plane stress conditions, *J. Mech. Phys. Solids*, **39**, 683-722.
- DENG X., ROSAKIS A. J., 1992a, A finite element investigation of quasi-static and dynamic asymptotic crack tip fields in hardening elastic-plastic solids under plane stress; Part I: Crack growth in linear hardening materials, *Int. J. Fract.*, **57**, 291-308.
- DENG X., ROSAKIS A. J., 1992b, A finite element investigation of quasi-static and dynamic asymptotic crack tip fields in hardening elastic-plastic solids under plane stress; Part II: Crack growth in power-law hardening materials, *Int. J. Fract.*, **58**, 137-156.
- DENG X., 1992c, The asymptotic structure of transient elastodynamic fields at the tip of a stationary crack, *MECH Report 92-4*, Department of Mechanical Engineering, University of South Carolina, Columbia, South Carolina, USA. To appear in *Proc. R. Soc. Lond. A*.
- DENG X., 1993, Transient, asymptotic, elastodynamic analysis: A simple method and its application to mixed-mode crack growth, *Int. J. Solids Struct.*, **30**, 513-519.
- FREUND L. B., DOUGLAS A. S., 1982, The influence of inertia on elastic-plastic antiplane-shear crack growth, *J. Mech. Phys. Solids*, **30**, 59-74.
- FREUND L. B., ROSAKIS A. J., 1992, The structure of the near-tip field during transient elastodynamic crack growth, *J. Mech. Phys. Solids*, **40**, 699-719.
- KALTHOFF J. F., 1983, On some current problems in experimental fracture mechanics, *Workshop on dynamic fracture* (KNAUSS W. G. et al., eds), California Institute of Technology, Pasadena, California, USA, 11-35.
- KALTHOFF J. F., BEINERT J., WINKLER S., 1980, Analysis of fast running and arresting cracks by the shadow-optical method of caustics, *Optical methods in mechanics of solids* (LAGARDE A., Ed.), IUTAM Symposium, University of Poitiers, France 1979, Sijthoff-Noordhoff, Alphen aan den Rijn, 497-508.
- KOBAYASHI T., DALLY J. W., 1980, Dynamic photo-elastic determination of  $\dot{a}$ -K relation for the 4340 steel, *Crack arrest methodology and applications*, ASTM STP 711, Ed. HAHN G. T. et al., American Society for Testing and Materials, 189-210.
- KRISHNASWAMY S., ROSAKIS A. J., 1991, On the extent of dominance of asymptotic elastodynamic crack-tip fields; Part I: An experimental study using bifocal caustics, *J. Appl. Mech.*, **58**, 87-94.
- KRISHNASWAMY S., ROSAKIS A. J., RAVICHANDRAN G., 1991, On the extent of dominance of asymptotic elastodynamic crack-tip fields; Part II: A numerical investigation of three-dimensional and transient effects, *J. Appl. Mech.*, **58**, 95-103.
- LAM P. S., FREUND L. B., 1985, Analysis of dynamic growth of a tensile crack in an elastic-plastic material, *J. Mech. Phys. Solids*, **33**, 153-167.
- LARSSON S. G., CARLSSON A. J., 1973, Influence of non-singular stress terms and specimen geometry on small-scale yielding at crack tips in elastic-plastic materials, *J. Mech. Phys. Solids*, **21**, 263-277.
- NIGAM H., SHUKLA A., 1988, Comparison of the techniques of transmitted caustics and photoelasticity as applied to fracture, *Exp. Mech.*, **28**, 123-133.
- NISHIOKA T., ATLURI S. N., 1983, Path-independent integrals, energy release rates, and general solutions of near-tip fields in mixed-mode dynamic fracture mechanics, *Engng. Fract. Mech.*, **18**, 1-22.
- MCCLEINTOCK F. A., 1956, The growth of fatigue cracks under plastic torsion, *Proceedings of International Conference on Fatigue of Metals*, The Institute of Mechanical Engineers, London, 538-542.
- MCCLEINTOCK F. A., 1958, Ductile fracture instability in shear, *J. Appl. Mech.*, **25**, 582-588.

- MCCLINTOCK F. A., IRWIN G. R., 1964, Plasticity aspects of fracture mechanics, *Fracture Toughness Testing and Its Applications*, ASTM STP 381, American Society for Testing and Materials, 84-113.
- NARASIMHAN R., ROSAKIS A. J., HALL J. F., 1987, A finite element study of stable crack growth under plane stress conditions: Part I—Elastic-perfectly plastic solids, *J. Appl. Mech.*, **54**, 838-845.
- ÖSTLUND S., 1991, Large scale yielding for dynamic crack growth in a strip geometry, *Int. J. Fract.*, **49**, 219-237.
- ÖSTLUND S., GUDMUNDSON P., 1988, Asymptotic crack tip fields for dynamic fracture of linear strain-hardening solids, *Int. J. Solids Struct.*, **24**, 1141-1158.
- PONTE CASTAÑEDA P., 1987, Asymptotic fields in steady crack growth with linear strain-hardening, *J. Mech. Phys. Solids*, **35**, 227-268.
- RICE J. R., 1974, Limitations to the small scale yielding approximation for crack tip plasticity, *J. Mech. Phys. Solids*, **22**, 17-26.
- ROSAKIS A. J., 1980, Analysis of the optical method of caustics for dynamic crack propagation, *Engng. Fract. Mech.*, **13**, 331-347.
- ROSAKIS A. J., DUFFY J., FREUND L. B., 1984, The determination of dynamic fracture toughness of AISI 4340 steel by the shadow spot method, *J. Mech. Phys. Solids*, **32**, 443-460.
- ROSAKIS A. J., LIU C., FREUND L. B., 1991, A note on the asymptotic stress field of a non-uniformly propagating dynamic crack, *Int. J. Fract.*, **50**, R39-R45.
- TIPPUR H. V., KRISHNASWAMY S., ROSAKIS A. J., 1991, Optical mapping of crack tip deformations using the methods of transmission and reflection coherent gradient sensing, *Int. J. Fract.*, **52**, 91-117.
- YANG L., DENG X., CHAO Y. J., 1993, *Explicit expressions of transient elastodynamic crack tip fields for mixed-mode crack propagation*, MECH Report 93-1, Department of Mechanical Engineering, University of South Carolina, Columbia, South Carolina, USA. To appear in *Engng. Fract. Mech.*
- ZEHNDER A. T., ROSAKIS A. J., 1990, Dynamic fracture initiation and propagation in 4340 steel under impact loading, *Int. J. Fract.*, **43**, 271-285.

(Manuscript received November 11, 1992;  
accepted December 14, 1993.)